Electronic Supplementary Material (ESI) for Molecular BioSystems.

SUPPORTING INFORMATION

Molecular Dynamics Investigations of Membrane-Bound CYP2C19 Polymorphisms Reveal Distinct Mechanisms for Peripheral Variants by Long-Range Effects on the Enzymatic Activity

YingLu Cui [a] *and Rongling Wu* *[a, b]

[a]Center for Computational Biology, College of Biological Sciences and Biotechnology, Beijing Forestry University, Beijing, 100083, China;
[b]Center for Statistical Genetics, The Pennsylvania State University, Hershey, PA 17033, USA

Correspondence: Professor R Wu, Center for Computational Biology, College of Biological Sciences and Biotechnology, Beijing Forestry University, Beijing, 100083, China. E-mail: rwu@phs.psu.edu

Figure S1. The overall structure of CYP2C19, colored from N-terminal (blue) to C-terminal (red).

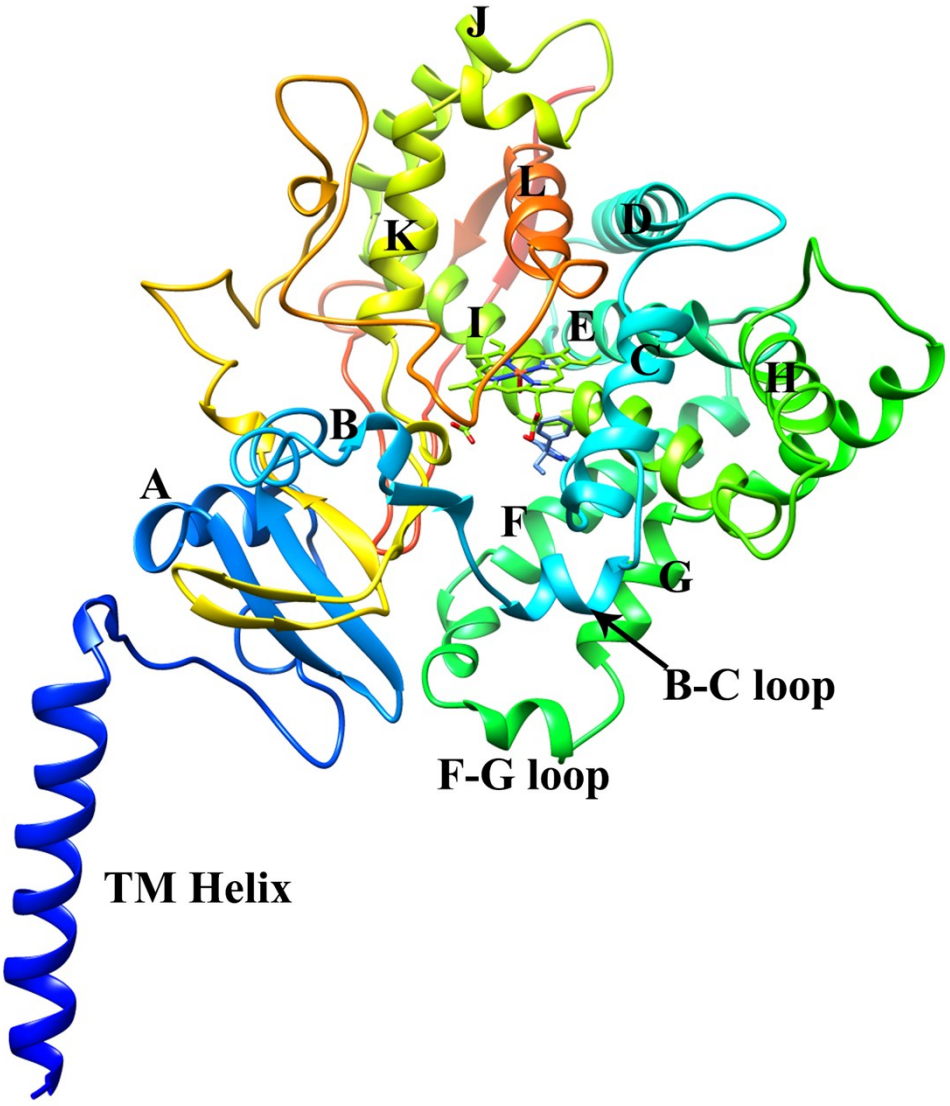

Figure S2. Secondary structure variation along the membrane-bound simulations of wt2C19 and two mutants. Residues in β-sheet, 3-10 helix, α-helix and Pi-helix are shown in green, blue, red, and orange respectively. Residues in non-regular or other secondary structure are shown in white. Conformational heterogeneity of the A161P and P227L mutants with respect to wt2C19 are shown in black and blue rectangles, respectively.

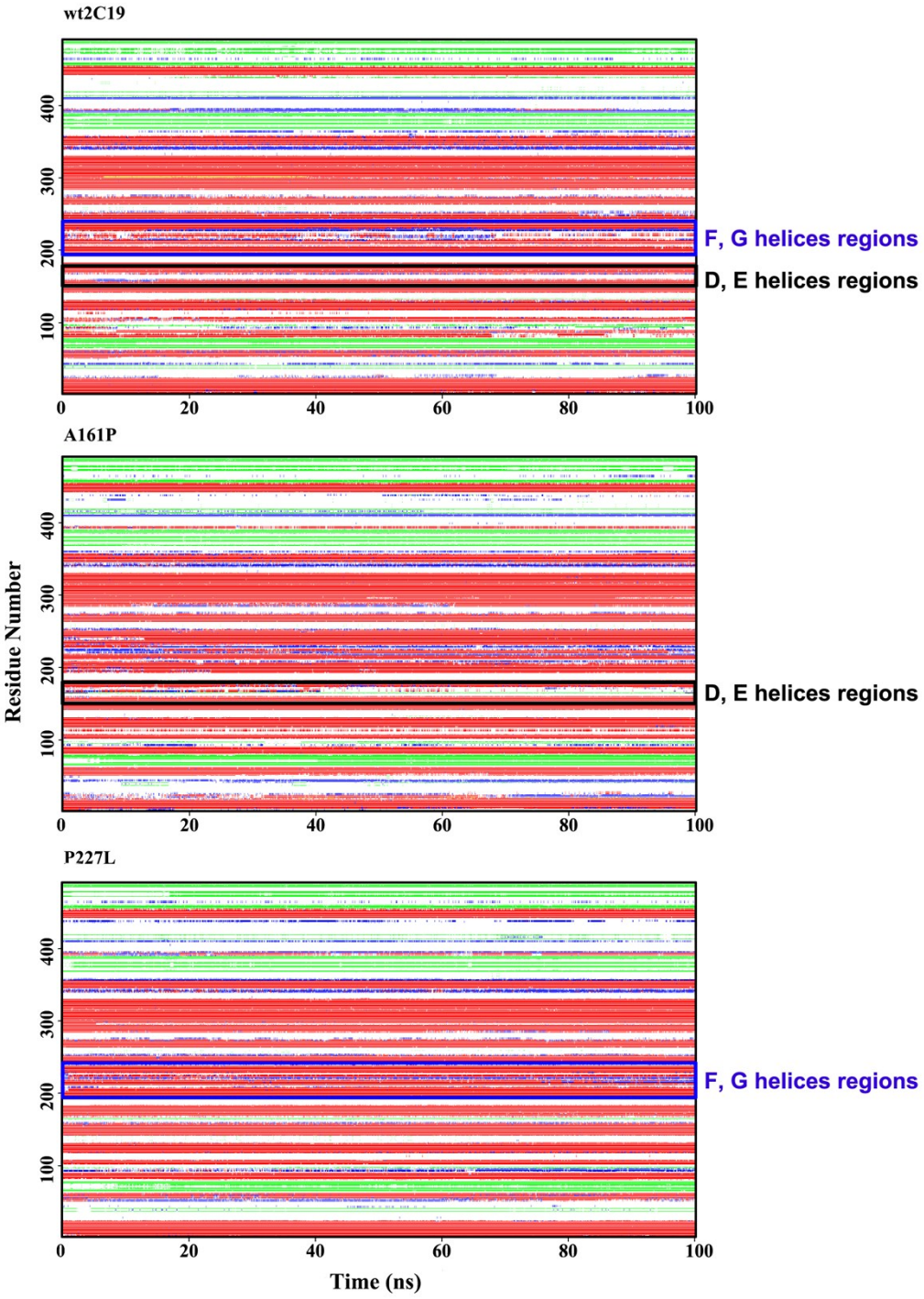

Figure S3. Time evolution of the short G' helix/refolded G helix (residues I222 to P/L227) along the z axis during the simulations of wt2C19 and P227L mutant. The heme plane was translated and rotated to coincide with the xy plane in advance to ensure the z coordinate of each projection point of heme to be zero.

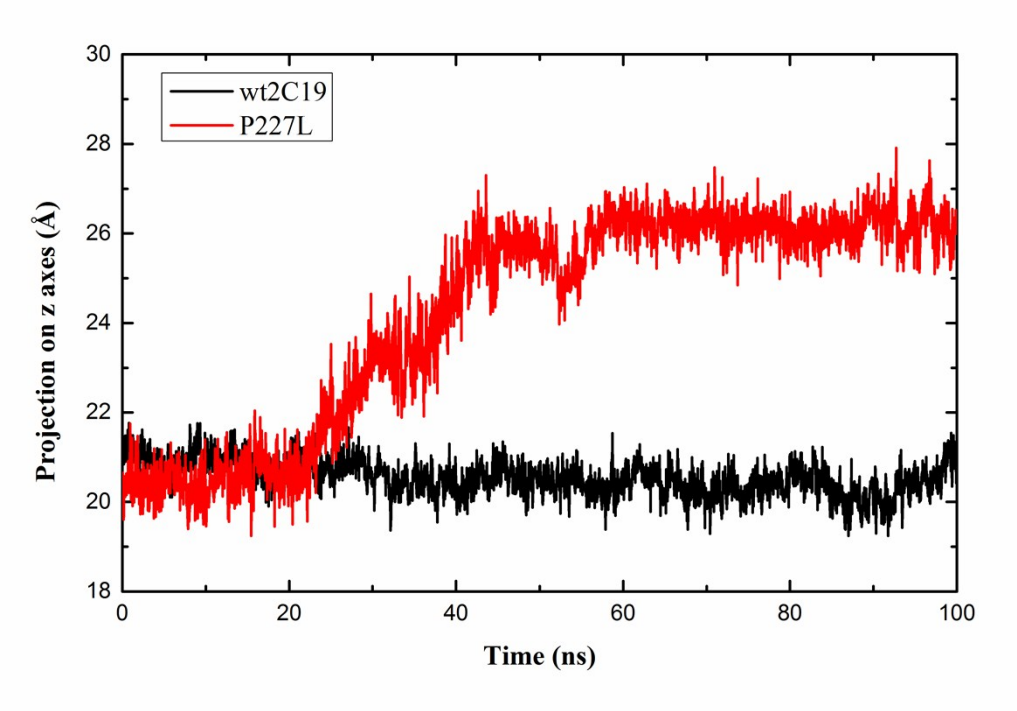

Figure S4. Key residues for S-mephenytoin binding of the representative structures of (A) wt2C19 (green), (B) A161P (blue), and (C) P227L (yellow) mutants. The residues and S-mephenytoin are shown in salmon and cyan sticks, respectively.

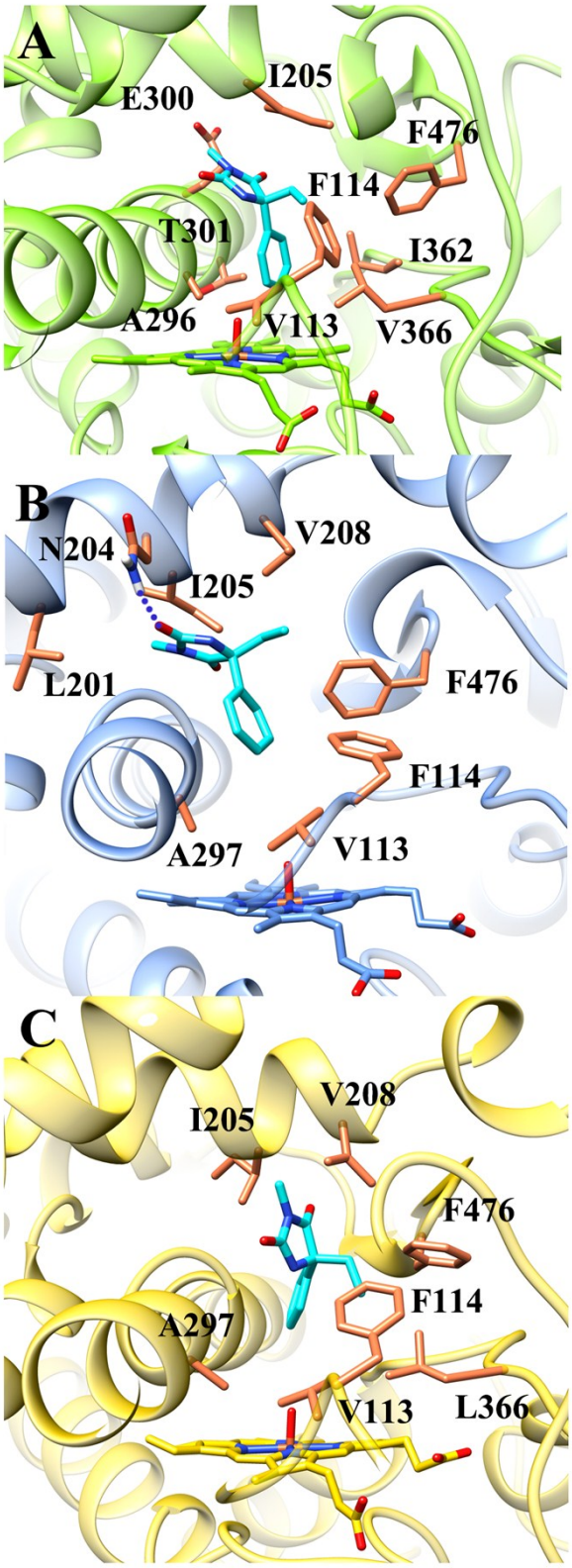

Table S1. Hydrogen bonds occupancies of the residues located on the specific regions for wt2c19, A161P, and P227L mutants

	H-bond	Occupied(%)		
	D, E helices regions	wt2C19	A161P	P227L
1	T159@O-S162@H	38.86	1.31	40.98
2	S162@OG-C164@H	24.42	NA	16.58
3	D165@OD1-T167@H	51.62	52.69	60.66
4	D165@O-F168@H	1.64	34.37	0.78
5	D165@O-I169@H	NA	21.42	NA
6	P166@O-L170@H	54.39	10.96	53.14
7	F168@O-G171@H	25.46	13.04	21.51
8	F168@O-C172@H	58.98	NA	57.84
9	I169@O-A173@H	44.50	18.65	49.46
10	C172@O-N176@H	51.24	14.12	58.30
11	C175@O-C179@H	67.59	36.82	67.82
	N terminal of the G helix			
1	I222@O-Y225@H	NA	NA	39.02
2	I222@O-F226@H	22.84	21.52	35.34
3	I222@O-P/L227@H	NA	NA	10.28
4	D224@OD2-R105@HH21	52.34	50.64	NA
5	F226@O-T229@H	8.58	11.22	26.75
6	F226@O-T229@HG1	38.58	35.78	7.32
7	F226@O-H230@H	NA	NA	45.26
8	P/L227@O-N231@H	53.96	49.38	43.86
9	G228@O-K232@H	47.52	33.22	30.25
10	T229@O-L233@H	9.26	NA	22.86
11	H230@O-L233@H	34.36	25.64	NA
12	N231@O-K235@H	59.56	57.50	60.21
13	K232@O-N236@H	50.46	53.66	64.69
14	L233@O-L237@H	38.38	34.46	42.06
15	L234@O-A238@H	65.88	61.74	60.97

Table S2. Characteristics of the top ranked pathways of CYP2C19 and its mutants

wt2C19

Pathway	2f	2a	5	2b	S
Occurrence[a]	72%	60%	55%	44%	49%
Mean bottleneck radius	1.75±0.23	1.74±0.32	1.73±0.31	1.64±0.10	1.44±0.17
Max. bottleneck radius [Å]	2.39	2.40	2.49	2.07	1.85

A161P

Pathway	2f	S	2a	2b	5
Occurrence[a]	73%	62%	47%	42%	40%
Mean bottleneck radius	1.71±0.17	1.73±0.25	1.63±0.11	1.56±0.17	1.58±0.12
Max. bottleneck radius [Å]	2.29	2.49	2.04	2.02	1.93

P227L

Pathway	2f	S	2b	2a	2e
Occurrence[a]	64%	55%	49%	44%	41%
Mean bottleneck radius	1.58±0.18	1.48±0.13	1.48±0.07	1.46±0.04	1.47±0.05
Max. bottleneck radius [Å]	2.05	1.96	1.87	1.82	1.84

Table S3. Decomposition of binding free energy (kcal mol^{-1}) on per-residue basis for wt2C19, A161P mutant and P227L mutant

(A) wt2C19

Residue	ΔE_{vdw}	ΔE_{ele}	ΔE_{GB}	ΔG_{SASA}	ΔG_{bind}
A297	-1.63	0.48	-0.12	-0.16	-1.43
L366	-1.10	-0.03	0.12	-0.14	-1.15
HEM	-1.70	-1.63	2.25	-0.04	-1.12
G296	-0.75	-0.91	0.72	-0.06	-1.00
I205	-0.93	0.02	0.03	-0.11	-0.99
E300	-1.07	0.24	-0.02	-0.12	-0.97
F476	-0.88	-0.34	0.47	-0.20	-0.95
T301	-0.54	-0.03	-0.08	-0.07	-0.72
V113	-0.77	0.26	0.06	-0.10	-0.55
F114	-0.42	0.08	-0.06	-0.11	-0.51
I362	-0.41	-0.04	0.01	-0.06	-0.50

(B) A161P

Residue	ΔE_{vdw}	ΔE_{ele}	ΔG_{GB}	ΔG_{SASA}	ΔG_{bind}
I205	-0.87	-0.03	0.01	-0.11	-1.00
A297	-0.86	0.17	-0.12	-0.09	-0.90
F476	-0.77	-0.24	0.31	-0.17	-0.87
G296	-1.51	-0.11	1.08	-0.29	-0.83
V208	-0.76	-0.07	0.18	-0.11	-0.76
N204	-0.88	-1.64	1.92	-0.13	-0.73
V113	-0.70	0.18	0.03	-0.12	-0.61
L201	-0.43	-0.19	0.04	-0.01	-0.59
F114	-0.48	-0.01	0.02	-0.08	-0.55
L233	-0.48	0.14	0.01	-0.09	-0.42
F100	-0.35	-0.04	0.01	-0.04	-0.42
HEM	-0.47	-1.19	1.28	-0.04	-0.42

(C) P227L

Residue	ΔE_{vdw}	ΔE_{ele}	ΔG_{GB}	ΔG_{SASA}	ΔG_{bind}
I205	-1.25	-0.03	-0.14	-0.19	-1.61
A297	-1.07	0.09	-0.06	-0.11	-1.15
V208	-1.11	-0.22	0.39	-0.18	-1.12
F476	-0.99	-0.20	0.28	-0.13	-1.04
L366	-0.95	0.03	0.09	-0.13	-0.96
HEM	-1.05	-1.73	1.94	-0.05	-0.89
G296	-1.23	-0.41	1.07	-0.22	-0.79
V113	-0.85	0.14	0.22	-0.14	-0.63
F114	-0.46	0.05	-0.04	-0.08	-0.53
I362	-0.40	0.01	-0.02	-0.07	-0.48
F100	-0.27	-0.04	-0.03	-0.02	-0.36
T301	-0.29	0.07	-0.07	-0.05	-0.34